ISSN 8755-6839

SCIENCE OF **TSUNAMI HAZARDS**

Journal of Tsunami Society International

Volume 35 **Number 3** **2016**

ASSESSING LANDSLIDE-TSUNAMI HAZARD IN SUBMARINE CANYONS, USING THE COOK STRAIT CANYON SYSTEM AS AN EXAMPLE

William Power
GNS Science, 1 Fairway Drive, Avalon, Lower Hutt, New Zealand
Joshu Mountjoy
NIWA, 301 Evans Bay Parade, Hataitai, Wellington, New Zealand
Emily Lane
NIWA, 10 Kyle Street, Riccarton, Christchurch, New Zealand
Stephane Popinet
Université Pierre et Marie Curie, 4 Place Jussieu, 75005 Paris, France
Xiaoming Wang
GNS Science, 1 Fairway Drive, Avalon, Lower Hutt, New Zealand

ABSTRACT

Tsunami generated by submarine landslides are now recognised as an important hazard, following several historical events. Submarine landslides can occur in a variety of settings such as on continental slopes, volcanic slopes, and submerged canyons and fjords. While significant progress has been made in understanding tsunami generation processes on open slopes, the problem of tsunami generation by landslides within submarine canyons has received less attention. In this paper we examine the tsunami hazard posed by submarine landslides in the Cook Strait canyon system, near Wellington, New Zealand. Understanding of the hazard posed by this tsunami source has practical value because of its proximity to a populated coast. Our studies also provide general results highlighting the differences between tsunami generation on open coasts and tsunami generation

within canyons. Geotechnical and geological studies of the Cook Strait region reveal evidence for many large landslide scars in the canyon walls, these are interpreted to be failures of consolidated material which descend the slopes on the sides of the canyon. Scouring of the base of the canyon slopes by strong tidal currents is believed to be an important process in bringing slopes to the point of failure, with most large failures expected to occur during earthquake shaking. We present the results of computer simulations of landslide failures using simplified canyon geometries represented in either 2D (vertical slice) or 3D. These simulations were made using Gerris, an adaptive-grid fluid dynamics solver. A key finding is that the sudden deceleration of the landslide material after reaching the canyon floor, leads to larger amplitude waves in the back-propagation direction (i.e. in the opposite direction to the initial landslide motion).

1. INTRODUCTION

Submarine landslide-generated tsunami are now a widely recognised hazard with documented historical events (Fine et al., 2005; Labbe et al., 2012; Rahiman et al., 2007; Tappin et al., 2008), landslide-specific hazard assessments (e.g. Argnani et al., 2011; Iglesias et al., 2012; Walters et al., 2006), and a limited number of regional hazard assessments (e.g. Grilli et al., 2009). Submarine landslides are recognised to occur in relatively specific geological environments, including open slopes, submarine canyons, fiords, and volcanic cones and ridges (Hampton et al., 1996). Submarine canyons are an environment where relatively few landslide studies have been carried out, yet where the hazard associated with landslide-generated tsunami may be high due to steep slopes, proximity to land, and the potential for landward-directed slope failures.

Whereas much of the world's landmass sits adjacent to a wide continental shelf, providing a buffer zone to continental slopes, submarine canyons enable areas of steeply sloping seafloor to come within close proximity of populated coastal areas. Examples of canyons in reasonably close proximity to populated areas can be found in Mediterranean Europe, Central eastern USA, and New Zealand. In comparison to open slopes, where landslide features are commonly beautifully preserved (e.g. Berndt et al., 2012), landslides in submarine canyons are frequently represented by relatively subtle geomorphic features (e.g. Greene et al., 2002; Lastras et al., 2007; Mountjoy et al., 2009). Landslides in submarine canyons typically occur on canyon walls and can be subject to geologically rapid post-failure modification, making them difficult to parameterise. In addition, failure often involves bedrock rather than recent sedimentary deposits adding additional complications for landslide analysis.

An important aspect of the submarine canyon geological environment in terms of landslide tsunami hazard is that material is falling into a confined seafloor environment, meaning that failed slope material and hydrodynamic disturbance is likely to interact with the complex terrain of the canyon system. Modelling of landslide-tsunami sources has predominantly considered material displaced down a planar slope with an unconstrained lower boundary (e.g. Ward, 2001; Watts et al., 1999). Applying this simplified source geometry to the complex terrain in submarine canyons may not be appropriate and could lead to failure to identify wave focussing areas, and under-estimation of the tsunami hazard.

Here we use a regional case study to explore the difficulties associated with landslide-generated tsunami hazard analysis in complex canyon terrain. The Cook Strait canyon system in New Zealand is a large submarine canyon that comes within 15 km of the capital city of Wellington, and has a large number of mapped submarine landslide scars (Micallef et al., 2012; Mountjoy et al., 2009). We present some results for this specific area regarding the age distribution of observed landslides, as this is a particularly difficult issue for landslide-tsunami hazard assessments. However the study is primarily focussed on identifying pitfalls for landslide-generated tsunami studies in submarine canyon terrain and suggesting a way forward for quantifying landslide tsunami hazard and risk in these complex environments.

We also present a modelling study into the tsunami-generation properties of landslides on canyon slopes, with particular regard for the differences compared to tsunami-generation on open slopes. The geometrical model of a submarine canyon that is used as the baseline for these studies is based on a simplified cross-section of part of the Cook Strait Canyon, yet is sufficiently generic to be used to draw general conclusions. Modelling was conducted using Gerris, a solver for the variable density Navier-Stokes equations, permitting more accurate fluid dynamics to be represented than can be achieved using standard depth-integrated tsunami models. The specific features of tsunami-generation by slope failures in canyon systems were investigated by varying the representation of the far wall, i.e. the slope opposite the mass failure, in the geometrical model of the canyon.

2. LOCAL SETTING

The seaway of Cook Strait divides North Island and South Island of New Zealand. The Cook Strait canyon system is a deeply incised submarine canyon formed on the continental slope of the southern Hikurangi Margin subduction system (Figure 1). The canyon is highly sinuous across the continental slope but branches into three canyon heads from the shelf break and extends 40 km across the continental shelf. Following Mountjoy et al (2013) the Cook Strait canyon system is divided into four components: the upper canyons - Cook Strait Canyon, Nicholson Canyon, and Wairarapa Canyon; and the Lower Cook Strait Canyon which extends from the shelf break to the deep sea Hikurangi Channel (Figure 1). In this study we focus on the upper, shelf-incising canyons as these are in shallower ocean depths, and come closer to land, meaning they are most likely to pose a tsunami hazard.

The head of Nicholson Canyon lies just 8 km off the coast of Wellington, New Zealand's capital city with a population of approximately 400,000. Wairarapa Canyon is just over 1 km from the coast at its closest point and all three of the upper canyons are less than 20 km from the coastline. The upper canyon rims vary in water depth from 50 – 200 m, and the canyon floor depths from 250 – 1200 m depth. The upper canyons are between 18 and 45 km long and 3 – 10 km wide.

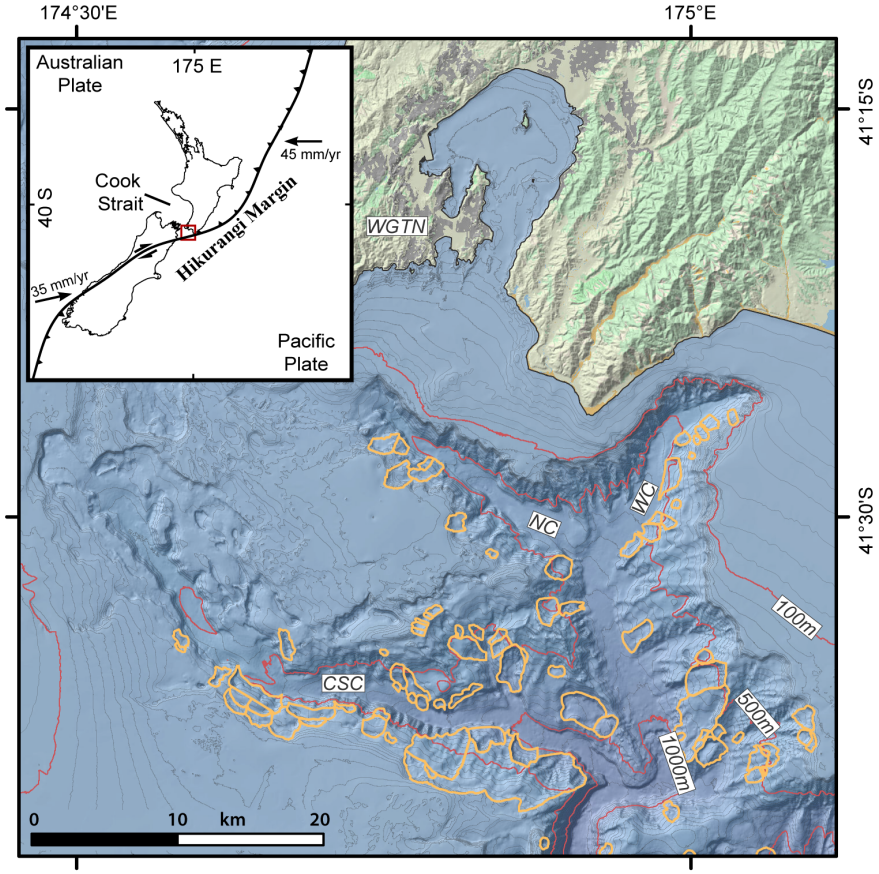

Figure 1. Regional setting. A) Study location in the context of the New Zealand tectonic setting. B) Canyon physiography showing mapped landslides (after Micallef et al. 2012). 'NC' is Nicholson Canyon, 'WC' is Wairarapa Canyon, 'CSC' is Cook Strait Canyon, and 'WGTN' labels the southern suburbs of Wellington City.

2.1 Tectonic and geologic setting

The Cook Strait canyon system sits at the southern termination of the Hikurangi Margin at the transition from subduction to continental collision on the Pacific-Australian plate boundary. Reflecting this active plate boundary setting, the region is dissected by numerous active faults that can be divided into reverse faults related to contraction in the convergent margin and strike slip faults from partitioning of oblique strain (Pondard and Barnes, 2010). In New Zealand's largest historical earthquake, the Wairarapa Fault ruptured in 1855 producing a Mw 8.2 earthquake centred onland and extending into the Nicholson and Wairarapa canyons (Barnes, 2005; Dowrick, 2005). Terrestrial seismic hazard assessments indicate that areas of the Wellington region are capable of producing peak ground accelerations (pga) greater than 0.4g at a 475 year return period, and they can exceed 1.0g at a 2500 year return period (Stirling et al., 2012). Earthquake ground shaking is thought to be the main trigger of slope failure within the canyon system (Micallef et al., 2012; Mountjoy et al., 2013).

2.2 Landslides in the Cook Strait Canyon System

130 landslides have been mapped through the Cook Strait canyon system (Figure 1). Landslides are recognised solely by scars in the canyon walls and canyon floor, as almost no evidence of landslide deposits remains in the system. Based on scar geometry, the metrics of the landslide source areas can be quantified in terms of key parameters like volume, failure depth and slope angle of the basal failure surface (Figure 2). These data indicate a predominance of landslides at volumes less than $10x10^6$ m^3, however a few failures are also above $1x10^8$ m^3. Frequency histograms of landslide depth have a peak between 70-90 m defining them as deep seated. The failure angle of the basal surface is predominantly controlled by bedrock structure and is mainly less than 10°, though it is likely that this value is overestimated as surficial material covering the landslide scar will skew results.

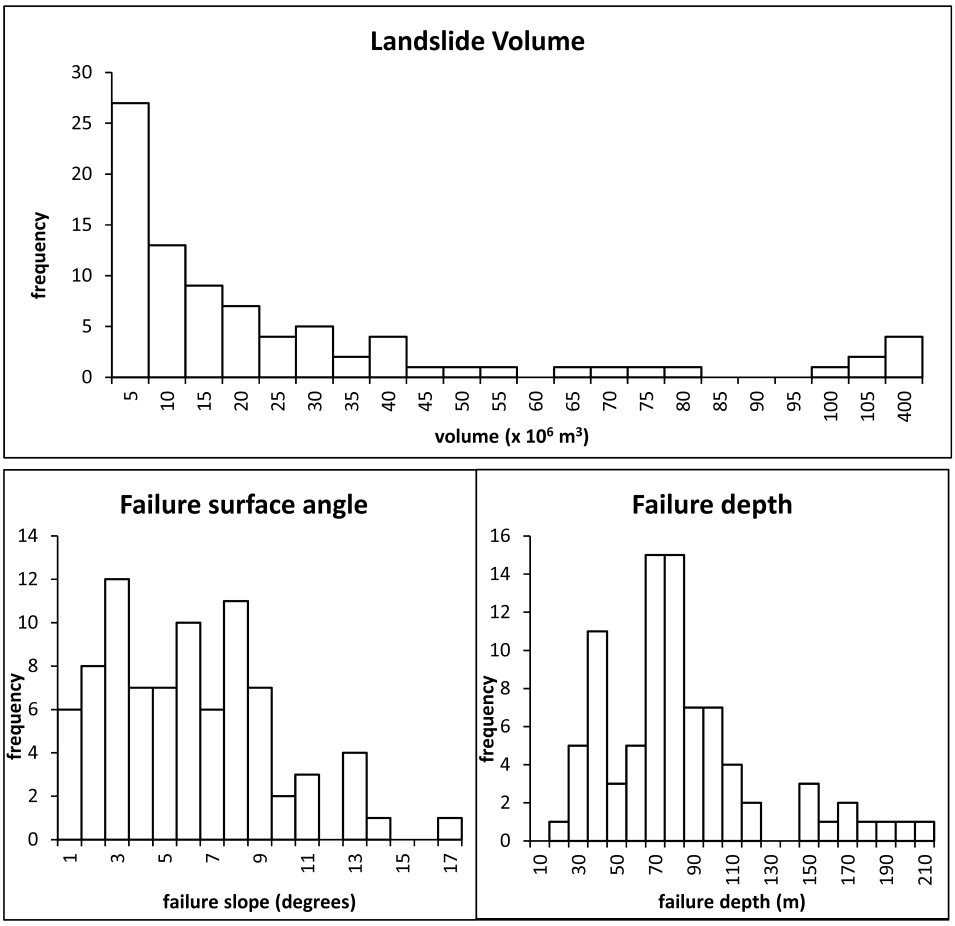

Figure 2. Landslides metrics after Micallef et al. (2012). Frequency histograms have been derived from measured geometries of landslide scars in multibeam bathymetry. Note the last bin for Landslide Volume is discontinuous in terms of scale.

3. DATA AND METHODS

3.1 Determining Landslide Age

Geophysical data and geological samples were collected in 2011 during the *RV Tangaroa* voyage Tan1103 (Mountjoy et al., 2013). Data relevant to this study was collected from several landslide scars within the canyon to assess the age of landslides (Table 2). Cores were collected with a standard gravity corer using a 6 m long barrel and a 1.2 tonne weight. Cores were capped and stored upright on-board then transferred to a refrigerated facility and logged onshore. Radiocarbon dating has been carried out on carbonate material (shell fragments or benthic foraminifera) picked from these sediment samples to determine sedimentation rates. The combination of sediment thickness and sedimentation rate data allow determination of the age of the surface underlying the sediment drape.

Digital high-resolution seismic data was collected using a hull-mounted Knudsen Chirp 3260 3.5 kHz Subbottom Profiler. Sub-bottom penetration was to a maximum of 60 m.

3.2 Modelling methodology

The modelling for this work took place in two parts. The first part investigated the process of the tsunami wave being created by the submarine mass failure, identifying general features that differentiate tsunamis caused by landslides in canyons from those on open slopes. This was done using modelling of simplified geometries in 2D (vertical slice) and 3D. The second part developed a scenario model specific to the Nicholson Canyon of Cook Strait, based on the actual seafloor bathymetry of this location and modelled the effect of that scenario.

The modelling was conducted using Gerris. Gerris is an extensible framework for the solution of partial differential equations describing fluid flows and other phenomena (Popinet, 2003). Gerris solves the variable-density Navier-Stokes equations with boundary conditions at the interface between phases, and uses adaptive mesh refinement to allow the model to adjust dynamically to the details of the problem being solved. For the purposes of long-range tsunami propagation modelling, Gerris can also solve the (depth-averaged) non-linear shallow water equations to simulate tsunami propagation over real bathymetry. The code is parallelised to enable speeding-up of expensive computations.

Navier-Stokes equation solver in Gerris was used to simulate the processes of landslide failure and wave generation at water surface in vertically 2D slice modelling and 3D modelling. Using a volume of fluid (VoF) approach, the air and water are represented by different phases of fluid. The landslide was modelled both as a third dense semi-rigid fluid. Solid boundaries were used at the edges of the domain for the VoF modelling. In the specific scenario the propagation of tsunami away from the source region was modelled with non-linear shallow water equation solver in Gerris using the water surface displacement and depth-averaged velocities from 3D modelling as initial condition. A subcritical boundary condition was used for sea boundaries allowing the tsunami energy to propagate out of the domain (Bristeau and Coussin, 2001).

3.3 Generalised landslide modelling

For the purposes of using a 2D vertical slice model to study the influence of canyon walls on tsunami generation, a baseline configuration was developed as shown in Figure 3. This geometry was based approximately on that estimated for past and future landslides in a cross-section of Nicholson Canyon. By modelling a landslide and subsequent tsunami in the baseline configuration, and then varying individual parameters, it was possible to estimate the sensitivity of tsunami wave generation to those parameters.

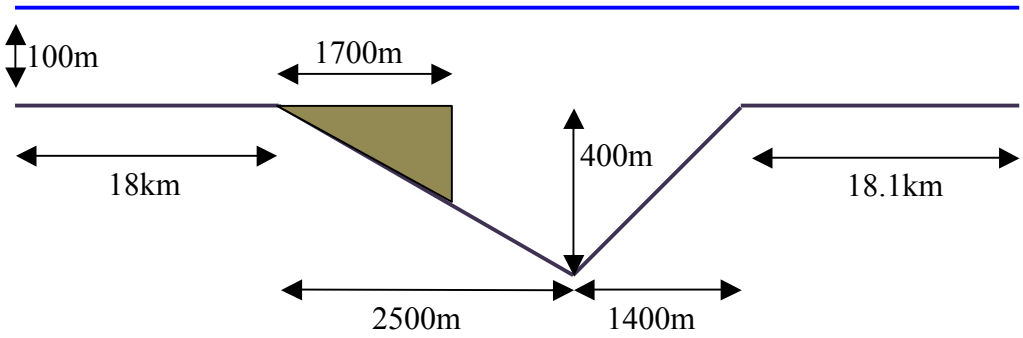

Figure 3. Baseline geometry used for modelling of a sliding block descending into a canyon. X co-ordinates in subsequent figures are measured relative to the position of the left post-landslide lip of the canyon.

For the purposes of this model it was assumed that the landslide material slides as a coherent block until the point where it hits the bottom of the canyon, after which it is assumed to behave as a dense fluid (due to break-up of the landslide body). This was achieved in Gerris by tracking the centre of mass motion of the slide and constraining the velocities in model-grid cells within the slide body to equal the centre of mass velocity until the canyon bottom was reached. The relative density of the landslide was assumed to be 2.0.

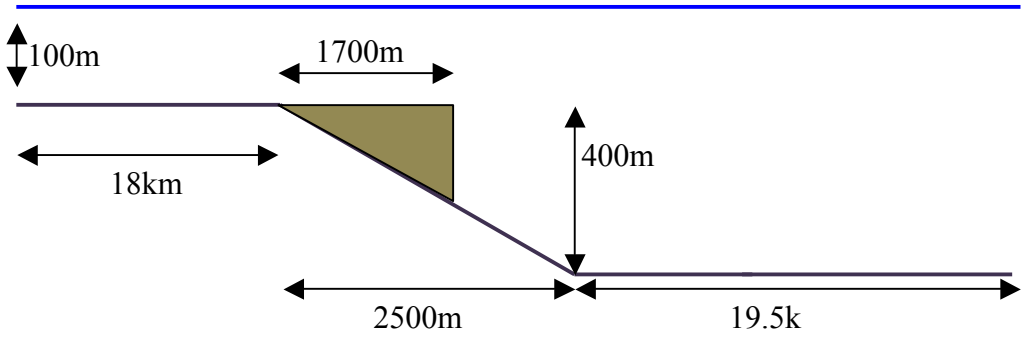

Figure 4. Geometry used for the models of a sliding block descending an open slope to a flat bottom. The influence of the far canyon wall was studied by constructing an alternative model in which there was no far wall, i.e. an open slope leading to a flat bottom. In this model the sliding block still descends as a solid body, but is assumed to become a dense fluid once it reaches the bottom of the slope.

A third configuration was also modelled in order to better understand the role of the far canyon slope. In this configuration the far wall is assumed to be almost vertical (Figure 5).

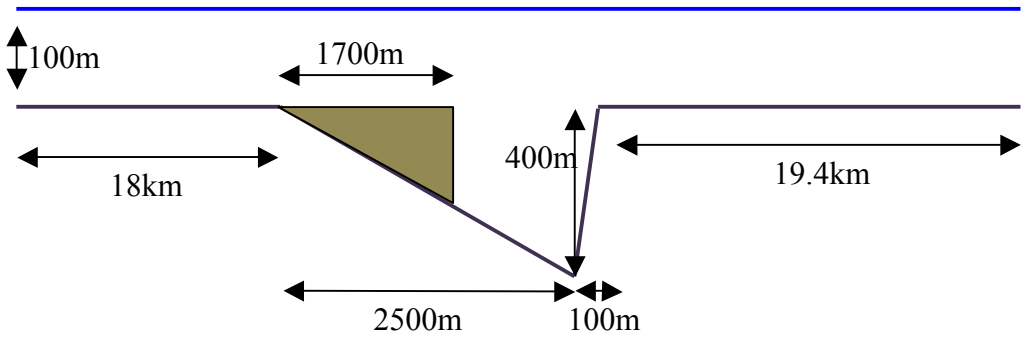

Figure 5. Geometry used for the models of a sliding block descending to a canyon with a very steep (near vertical) far wall.

Equivalent 3D simulations were conducted to investigate the effect the finite width of the landslide has on tsunami wave created. Figure 6 shows the configuration modelled. The cross-sections of the landslide and canyon remains the same as the baseline shown in Figure 3. However the landslide has

a finite width while the canyon extends unchanged in both directions.

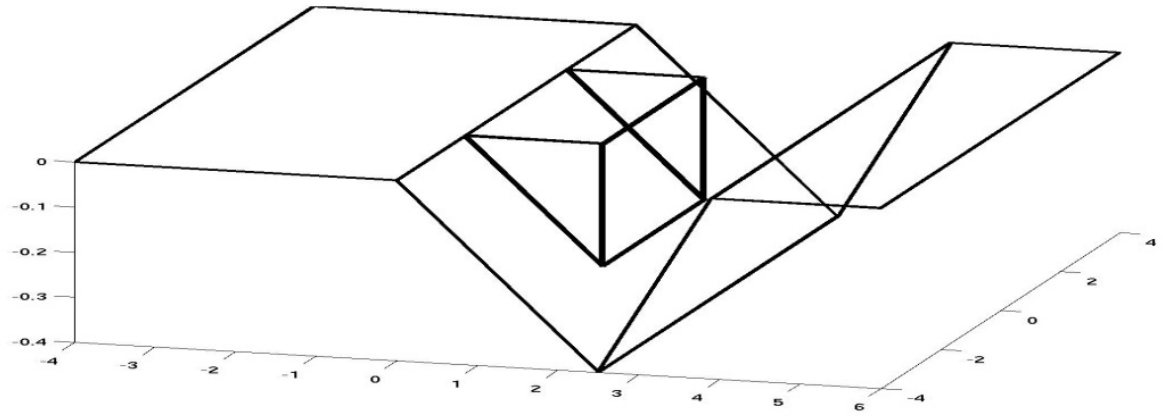

Figure 6. Three dimensional equivalent of baseline landslide geometry (Figure 3), dimension labels are in km. For the baseline 3D scenario the width of the slide, along the canyon axis, was 1.7km, in cross-section (perpendicular to the canyon axis) the dimensions are the same as in Figure 3.

The width of the landslide was varied from 1km, to 1.7km, to 2.5km and separate simulations made for each case, in order to understand how the validity of the 2D approximation varies according to the width of the slide. Watts et al (2005) discuss approaches for approximating 3D models with 2D vertical slice models, these use functions of the slide width to correct for the radiation in off-axis directions.

3.4 Cook Strait landslide modelling

In Section 2 potentially tsunamigenic submarine landslides within the Cook Strait region were identified. An estimate of the likely worst case scenario, in terms of overall impact on people and the built environment, in this region was identified as being caused by a landslide on the south side of Nicholson Canyon. The head of this canyon lies within 10 km of Wellington (see Figure 1). Table 1 shows the parameters used for modelling of this scenario.

Slide Parameters	**Nicholson Canyon**
Latitude (^{0} N)	-41.46
Longitude (^{0} E)	174.8
Azimuth (^{0})	50
Depth (m)	250
Slope (^{0} down from horizontal)	11.31
Length (m)	1500
Width (m)	1500
Thickness (m)	200
Volume (km^3)	0.4
Relative Density	2.0

Table 1. Parameters used in 3D initialisation of the Nicholson Canyon scenarios

This scenario was modelled in 3D as a rigid descending block, similar to that in Figure 6, which becomes a dense fluid after reaching the bottom of the canyon. After 100 seconds of modelled time had elapsed the water surface state and the depth-integrated velocity were used to form inputs to the non-linear shallow-water equation tsunami propagation model. Bathymetric and topographic data for this model were compiled from Land Information New Zealand bathymetric charts and ?.

4. RESULTS

4.1 Landslide age models

To get the required magnitude frequency model for landslide occurrence the most difficult aspect is determination of the frequency with which landslides occur. Whereas tectonic faulting is a repeated process over longer time periods mass instability is more of a stochastic process being dependant on many different local and external forcing factors. Any model for landslide recurrence requires some validation of the determined age model. A first order validation for this is the known ages of prior landslides, giving an indication that landslides are occurring over short enough timescales to pose a hazard.

To provide some validation that there is a landslide tsunami hazard associated with the Cook Strait Canyons we have analysed data from four separate landslides to get an idea of the age population of the landslides observed in geomorphology.

4.2 Radiometric dating results

Benthic Foraminifera and shell fragments extracted from sediment near the base of sediment cores have been dated using c14 radiometric dating techniques (Table 2). A local, averaged sediment accumulation rate is calculated between the seafloor (t=0) and the depth of the dated horizon. Other radiocarbon analysis in the Cook Strait canyons (Mountjoy et al., 2013) has shown that dating of foraminifera is unreliable for definite ages, likely due to both the lack of hemipelagic material and reworking of foraminifera material. However dates provide a maximum for stratigraphic ages as material cannot be older than the reported age but could be younger if reworked.

Table 2: Landslide dating data

Core ID	Date depth	C14 date (yrs BP)	Cover depth	Landslide age (yrs BP)
Stn 18	1.8 m	14217 +/- 127	NA	14217 +/- 127[1]
Stn 32	2.7 m	1031 +/- 85	6.96 +/- 0.2 m	2658 +/- 295
Stn 37	2.5 m	159 +/- 79	3.2 +/- 0.2 m	204 +/- 125
Stn 42	2.4 m	1470 +/- 75	5.84 +/- 0.2 m	3090 +/- 486

[1]The calibrated age is for material from sea level lowstand, which agrees with relict shell hash material observed in core. This age is applied to the landslide scar with no assumption of accumulation rate.

4.3 Subsurface imaging

To determine the amount of sediment that has been placed over the evacuated landslide scars since failure occurred we analyse high resolution (3.5 kHz) seismic reflection data. The example shown in Figure 8 illustrates the thin sediment drape overlying a landslide scar in Wairarapa Canyon.

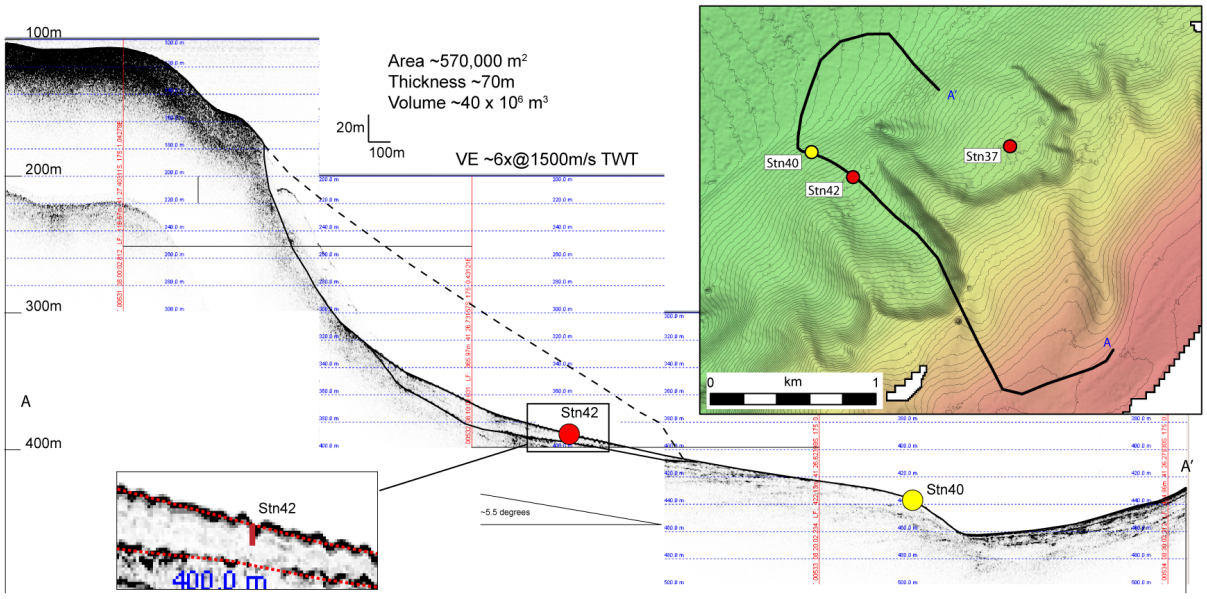

Figure 8. Example of date extrapolation through cover sequence to date landslide in 3.5 kHz seismic reflection. Dashed black line shows interpreted pre-failure geometry of slope. Inset detail shows cover sequence (red dash line) and penetration depth of core at Stn42.

The accumulation rate for this location in Table 2 is extrapolated to the full thickness of sediment overlying the landslide failure surface to determine the age of the scar (Table 2). Age uncertainty takes into account C14 dating error and measurement error in picking seismic horizons. Issues with this landslide age determination technique include inherited age in sediment (date is for older material transported from somewhere else), variation in sedimentation rates, the possibility of a polyphase landslide mechanism, and velocity variation in seismic depth conversion. In this case, the proximity of the adjacent much younger landslide (Stn37) with a very similar geomorphology suggest that the landslide illustrated in Figure 8 may be younger than the dating suggests. Regardless these age determinations indicate a range of post-glacial (20,000 BP) ages for the landslides in the canyon system.

4.4 Tsunami Modelling of canyon landslide in vertical cross-section

2D tsunami wave generation was modelled as described in Section 3 for the three cases of the baseline canyon, the open slope, and the vertical far wall, as shown in Figures 3, 4 and 5 respectively.

Results from these simulations are shown in Figures 9 and 10. Figure 9 shows the water surface at 100 second intervals following the landslide initiation. Figure 10 shows the water level time history above a point 4km from the canyon rim on the 'near' side (i.e. X=-4000 m, to the left of the canyon rim as it appears in Figures 3,4,5).

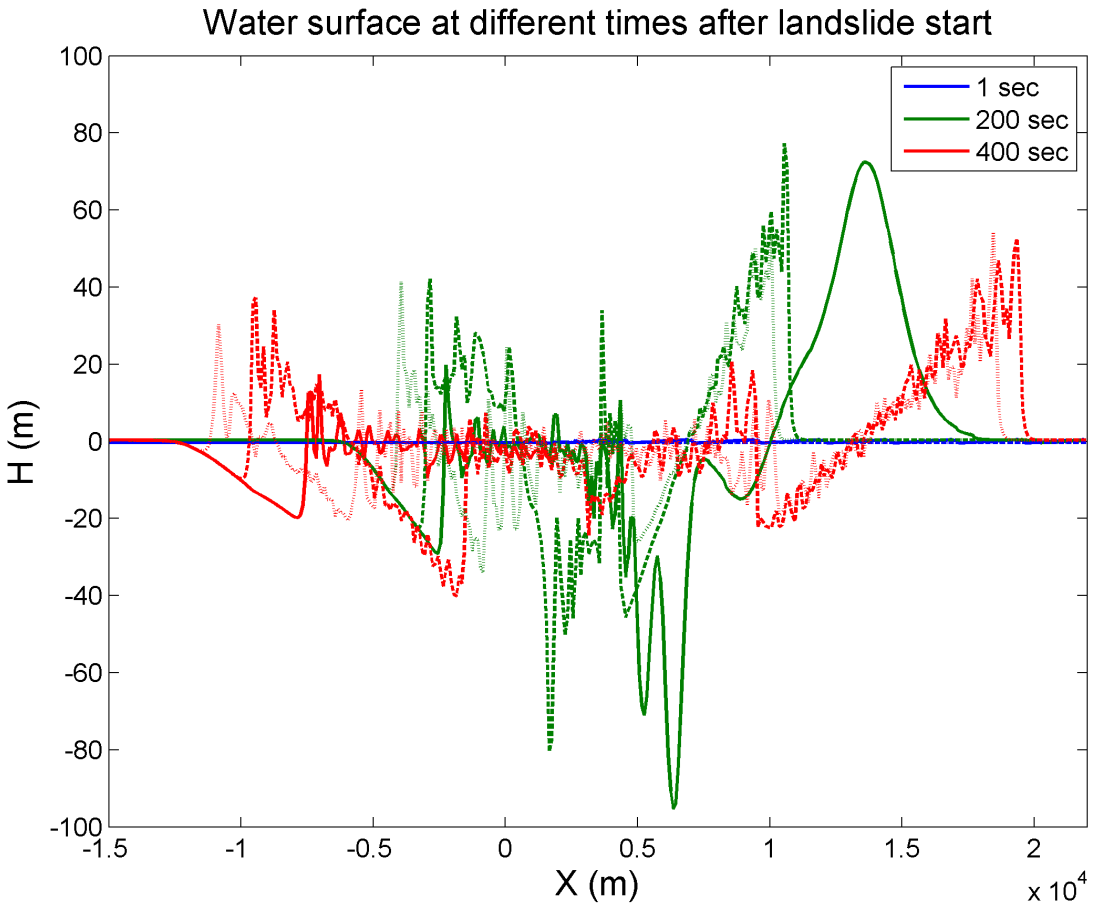

Figure 9. Water surface snapshots at 200 second intervals after landslide initiation, shown for the three geometric configurations described in the text: no-far wall (solid), the baseline canyon cross-section (dashed), and the very steep far-wall canyon (dotted). The no-far-wall case is not shown for +ve X at t=400 s; this is to avoid unrealistic effects caused by reflections from the edge of the simulation domain.

From Figure 9 we can see that the leading positive wave on the 'near' side of the canyon comes progressively earlier as we go from having a steep far wall to the baseline canyon to having no far wall. This suggests the timing of the first positive wave is related to the deceleration of the descending body. On the 'far' side of the canyon the leading wave, which is positive, travels faster in the absence of the far wall – which is to be expected given that tsunami wave speed is greater in water of greater depth.

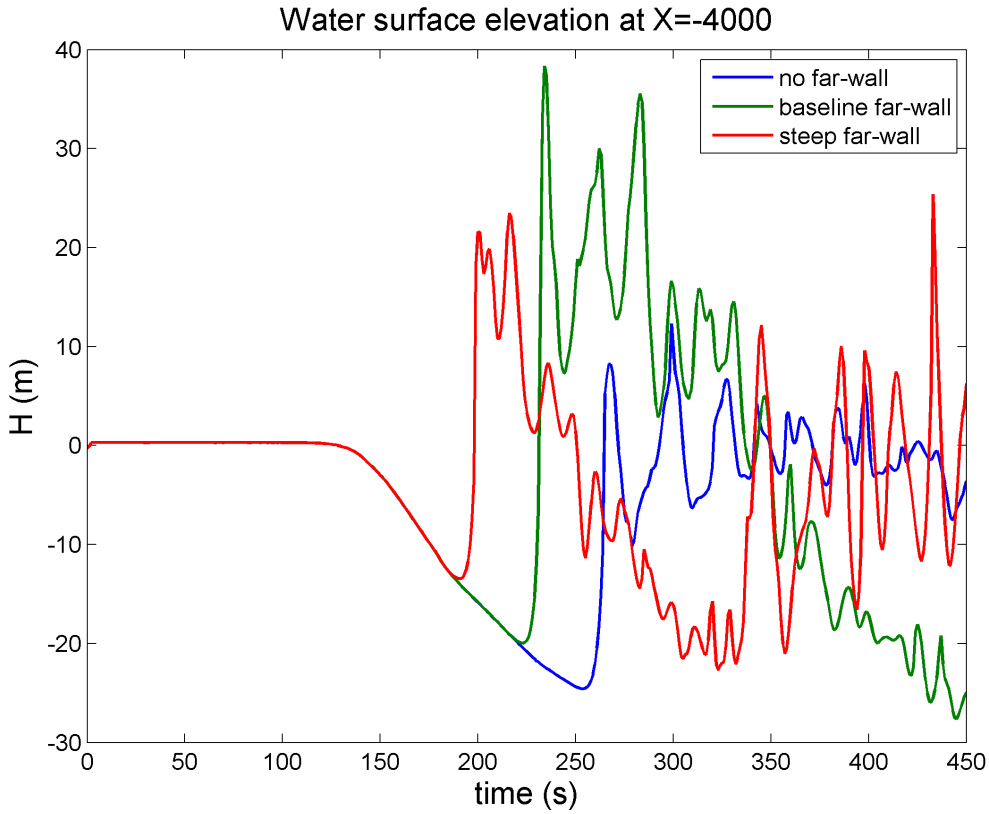

Figure 10: Water surface time histories at position X=-4000 m, shown for the three geometric configurations described in the text: no-far wall (blue), the baseline canyon cross-section (green), and the very steep far-wall canyon (red).

Analysing Figure 10 we see that the presence of the far canyon wall makes a big difference to the amplitude of the subsequent wave on the 'near' side of the canyon. In this example the elevation of the peak of the wave is about three times greater in the canyon geometry compared to the open slope case; this dramatically highlights the differences between tsunami generated by landslides in the two situations, and why it is important for hazard assessment not to model canyon landslide tsunami sources using procedures and approximations that assume an open slope. The role of landslide deceleration on tsunami generation has also been studied in laboratory experiments by Sue et al (2011).

4.6 Relationship between 2D and 3D models of canyon landslides

Two dimensional vertical slice (2D) modelling is significantly less demanding of computer time than fully three dimensional (3D) modelling. Hence it is useful to evaluate the differences in results for equivalent scenarios in these two cases. Results of such a comparison appear in Figure 11. Here the 2D wavefield along the axis of the cross-section is compared against the equivalent 3D model for

landslides of different width in the along-canyon direction. What we see is that the 2D model overestimates the wave heights compared to the 3D case, as would be expected due to the finite width of the landslide in the 3D case as energy is radiated in the off-axis directions. The degree of overestimation reduces as the landslide width (in the canyon axis) increases. Ultimately, for a theoretical infinitely wide landslide, the two results should converge.

Qualitatively the 2D and 3D solutions show the same basic features. The question of how a 3D profile may be generated from a 2D cross-sectional model has been studied by Watts et al. (2005), such a solution has the potential to save much computer time in situations where many scenarios need to be modelled.

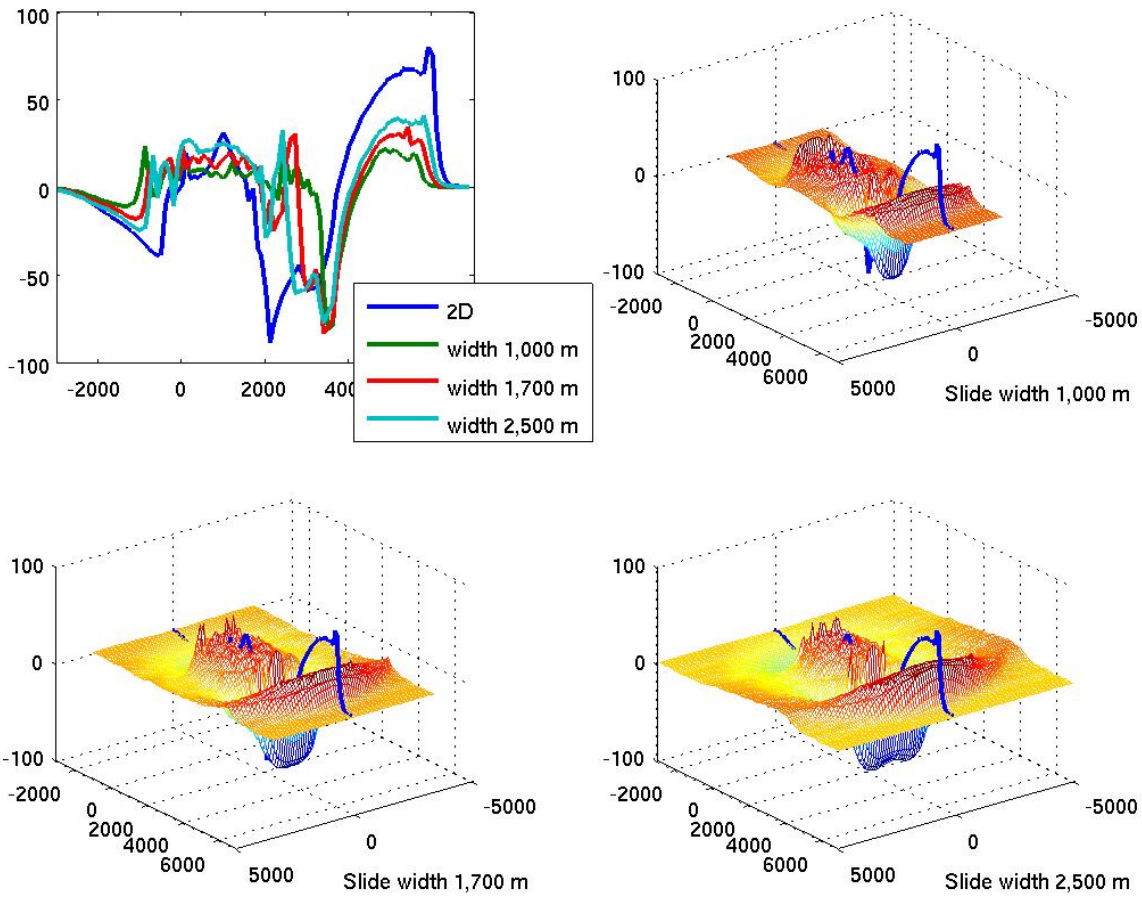

Figure 11: Comparing two-dimensional and three-dimensional modelling of tsunami generated by landslide in simplified bathymetry as given in Figure 7.2. All figures are taken at t = 100 s. Top left: vertical slices through y=0 for landslides with widths 1,000 m, 1,700 m and 2,500 m as well as two-dimensional vertical slice case. Top right: width = 1,000 m; bottom left: width = 1,700 m; bottom right: width = 2,500 m.

4.7 Cook Strait modelling scenario model

Maximum water levels produced from the Cook Strait tsunami propagation model initialised by the water level and velocity data produced from the 3D landslide model (see Section 3.4) are shown in Figure 12. We see that areas on the south coast of the North Island, close to the Wellington Harbour entrance, are estimated to experience tsunami waves with crests that approach or exceed 5m above the background water level in such a scenario.

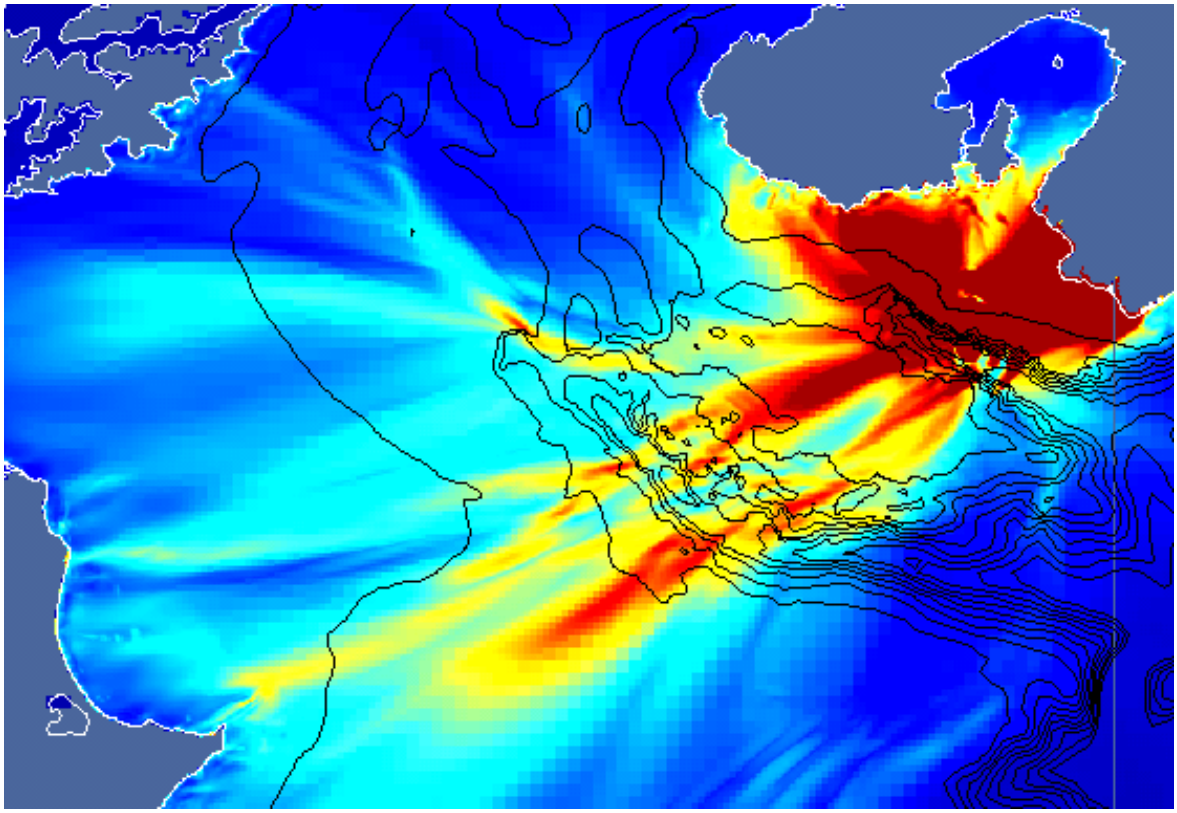

Figure 12. Maximum water levels (relative to background) in Cook Strait over the 3 hour period following the tsunami-initiating landslide in the Nicholson Canyon scenario. The colour scale ranges between 0 (dark blue) and 5 m (dark red).

These results demonstrate that there is a hazard to Wellington and the Cook Strait region in general from landslide-caused generated tsunami. While it is a long-term goal to incorporate landslide tsunami sources in a probabilistic hazard framework (See Section 5), it is useful at this time to place these events in context with other potential sources of tsunami in this region. Tsunamis of broadly similar size (~5m amplitude) may be caused by surface deformation alone during upper plate fault ruptures in the Cook Strait region, and larger tsunamis may be caused by earthquakes on the Hikurangi subduction interface, especially if such earthquakes rupture beneath Cook Strait (Cousins et al, 2007). Further, the modelled landslide was at the upper end of the volume distribution of observed

landslide scars, and was placed at the worst possible location. The infrequency with which such large landslides appear to occur, relative to the estimated frequency of earthquakes in this region (see e.g. Power, 2013), suggests that co-seismic deformation is probably the dominant contribution to tsunami hazard here.

5. DISCUSSION

5.1 Conceptual framework for building a landslide probability model

Any multi-source landslide-tsunami hazard model requires an underlying model of some form of magnitude frequency relationship defining when/how often landslides occur and their tsunami generating characteristics. A generalised magnitude frequency curve is shown in Figure 13. Landslides in submarine canyons likely occur from frequent very small events (sub resolution for ship-borne data collection) to infrequent events approaching cubic kilometre scale. The region of this curve that is of concern in terms of risk assessments however is limited to the central zone where landslides are large enough to generate hazardous tsunami, yet occur regularly enough to pose a risk. Defining the form of such a curve validated for a real world situation is a difficult task.

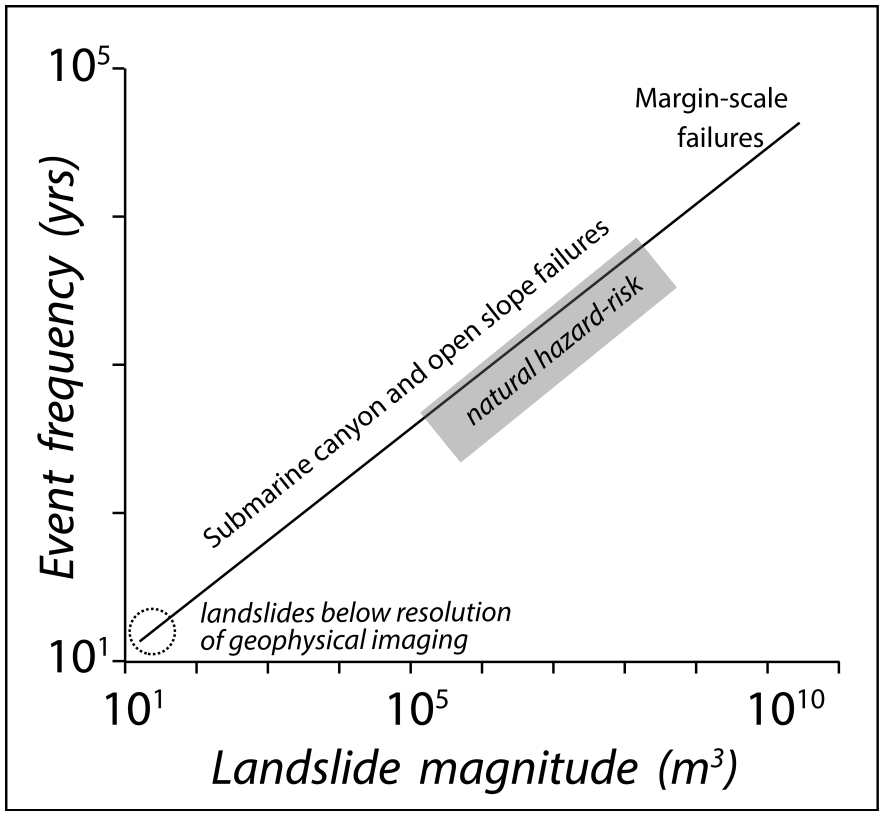

Figure 13: Conceptual magnitude frequency plot for landslide recurrence in continental margin settings.

We consider two approaches to defining magnitude frequency relationships for landslides in submarine canyon settings that could be used to underpin hazard and risk assessments.

5.2 Stability modelling approach – an assumption of earthquake triggering

In deep marine settings, and particularly those that also have an active tectonic setting, the majority of submarine landslides are inferred to be triggered by earthquakes (e.g. Sultan et al. 2004). While it is also acknowledged that many other processes influence slope stability, including: sediment loading, storm/wave loading, fluid/gas pressure/migration and slope erosion (Locat and Lee 2002). Many of these processes are factors that (pre) condition the slope for failure and do not necessarily trigger actual slope failure without additional external loading (e.g. a seismic load). The majority of submarine landslide studies, including those on passive and glaciated margins, invoke/infer earthquakes as the ultimate triggering mechanism in the absence of evidence for other specific mechanisms.

Based on this assumption it is possible to calculate the threshold level of earthquake shaking required to trigger failure and compare this against known return intervals for earthquake ground motion (e.g. Ten Brink et al 2009 Assessment of tsunami hazard to the U.S. East Coast Marine Geology 264A) (Strasser et al., 2007). This can be achieved via simple limit equilibrium calculations for slope stability, however the controlling parameters for such a model (e.g. mechanical strength, slip surface orientation) are not so easy to determine over large complex areas. Some approaches to this problem have been made, for example Ten Brink et al (2009) use a database of surface sediment samples correlated to mechanical parameters and infer vertical homogeneity. The authors acknowledge that this may not be applicable to areas such as submarine canyons where older consolidated rocks occur near or at the seafloor and exert a controlling influence on slope stability. In the submarine canyon case the problem is further complicated by the need to consider bedrock structure controls on slope failure, which is unlikely to be apparent from bathymetry alone.

In Cook Strait it is apparent that large landslides are controlled by bedrock orientation, in that they preferentially occur on bedding plane surfaces (Mountjoy et al., 2009). Given the lack of appropriate penetration and resolution subsurface imaging (multichannel seismic reflection data) it is very difficult to develop a regional model for failure orientation, bearing in mind that contrary to shallow rotational failures the seafloor gradient does not determine the failure plane gradient. As limit equilibrium models are very sensitive to failure plane gradient this is an important parameter. Based on the population of landslides it is possible to determine geometrical parameters for landslides (Figure 2), and these can be extrapolated to define the failure gradient over the extent of the study area given an appropriate population of landslides. Other key parameters such as failure depth may also be extrapolated from the landslide population.

The remaining key parameters that cannot be derived from the landslide population are the material properties. In all likelihood it will be necessary to infer properties based on studies of similar

rock and sediment from elsewhere. To accommodate the uncertainty inherent in this approach it is recommended that stability modelling is carried out via probabilistic (e.g. Monte Carlo) methods incorporating the appropriate range of values.

5.3 Landslide population approach – trigger independent

An alternative approach to this problem, that avoids the need to attain a thorough database of physical properties, is to develop an age model for observed landslides within a landscape. A regression of the landslide volume distribution presented in Figure 2 provides a magnitude distribution that determines the x-axis of the conceptual curve in Figure 12. While we do not have direct evidence for the age of more than four of these failures, the time period over which these landslides has occurred can be reasonably inferred. During sealevel lowstand periods the erosion and sediment deposition within most global canyon systems is enhanced, and this is expected to be the case for Cook Strait (Mountjoy et al., 2009). Thus we expect that the evidence for landslides observed in the canyons post-dates the start of sea-level rise, giving a maximum time period of 20,000 years. The dates presented in Table 2 do not contradict this. In fact it is possible that most landslides have occurred in the Holocene (post 10,000 years) and this may be a lower bound. This information can be used to develop a magnitude frequency curve of the form in Figure 12 that can be used to directly drive a landslide-tsunami hazard model. We do not present such a curve for Cook Strait as this study is meant as a general treatise on the generic issues associated with landslide-tsunami hazard assessments across submarine landslides rather than a specific case study. A magnitude frequency curve for submarine landslide occurrence may be used to directly control a probabilistic tsunami-hazard assessment. Alternatively it may be used to validate the results of a stability modelling based approach to assessing landslide recurrence.

Quantifying the likelihood of landslide occurrence in large submarine canyons is an inherently difficult problem. Although they are a first-order mechanism for the formation of the canyons, they are typically only identified by a scar in the canyon wall, with evidence for the deposit being removed. The concentration of currents and other erosion mechanisms means that the morphology of scars may be rapidly modified. Despite these difficulties, submarine canyons are one of the main mechanisms by which large and steep submarine slopes are able to come within close proximity of the land and human populations. This makes them very important in terms of natural hazards and demands that the issues and uncertainties associated with quantifying these hazards be overcome.

5.4 Effect of complex terrain on landslide-generated tsunami

A landslide into a canyon differs in the way it generates a tsunami compared to an equivalent landslide on an open slope. One difference is that the motion of the landslide body is suddenly decelerated, and rapidly brought to a halt or even reversed, by interaction with the slope of the

opposite canyon wall. Another difference is that tsunami waves generated by the landslide are themselves modified by the bathymetric features of the canyon – partial wave reflection may take place at the canyon walls, and the substantial differences in depth between the canyon floor and the surrounding continental shelf will affect the timing and refraction of the wave. Our results demonstrate that these influences can be significant, and that tsunami hazard assessments involving canyon systems will be more accurate if these effects are taken into consideration, rather than using methods that assume an open slope.

6. CONCLUSIONS

From the studies presented here we draw the following conclusions:

- Tsunami generation by submarine landslides in canyon systems is distinctly different to tsunami-generation by open coast landslides.
- Tsunami generation by submarine landslides in canyon systems is influenced by the sudden deceleration of the landslide at the bottom of the canyon, and this can lead to significantly larger waves in the opposite direction to the initial landslide motion.
- Tsunami-propagation within canyon systems is influenced by the bathymetry of the canyon which changes the wave speed, and hence causes refraction.
- The Cook Strait canyon system shows evidence for at least 130 landslides large enough to be mapped, and the majority of these are believed to have occurred in the Holocene (within the last 10,000 years).
- Landslides on the walls of the Cook Strait canyons predominantly occur in consolidated rock, rather than in accumulated sedimentary material as is typical of submarine landslides in depositional environments.
- Submarine landslides in the Cook Strait canyon system pose a risk to the city of Wellington in New Zealand, and it is likely that canyon systems elsewhere in the world pose similar risks to nearby coasts.

ACKNOWLEDGEMENTS

The authors would like to acknowledge helpful discussions with Christof Mueller and Phillip Barnes. This work was supported by the New Zealand Natural Hazards Platform (contract 2012-NIW-03-NHRP), and by GNS Science as part of its Government-funded, core research. This research was originally presented at the Tsunami Society 6th International Tsunami Symposium in Nicoya, Costa Rica.

REFERENCES

Argnani, A., Tinti, S., Zaniboni, F., Pagnoni, G., Armigliato, A., Panetta, D., and Tonini, R., 2011, The eastern slope of the southern Adriatic basin: a case study of submarine landslide characterization and tsunamigenic potential assessment: Marine Geophysical Research, v. 32, no. 1-2, p. 299-311.

Barnes, P. M., The southern end of the Wairarapa Fault and surrounding structures in Cook Strait, *in* Proceedings The 1855 Wairarapa Earthquake symposium, Wellington, 2005.

Berndt, C., Costa, S., Canals, M., Camerlenghi, A., de Mol, B., and Saunders, M., 2012, Repeated slope failure linked to fluid migration: The Ana submarine landslide complex, Eivissa Channel, Western Mediterranean Sea: Earth and Planetary Science Letters, v. 319, p. 65-74.

Bristeau, M.-O. and Coussin, B., 2001, Boundary conditions for the shallow water equations solved by kinetic schemes, Report RR-4282, INRIA Rocquencourt, Le Chesnay, France. Available online from http://www.inria.fr/rrrt/rr-4282.html.

Cousins, W. J., Power, W. L., Destegul, U. Z., & King, A. B., 2007, Combined Earthquake and Tsunami Losses for major earthquakes affecting the Wellington Region. GNS Science consultancy report, 280.

Dowrick, D. A., Strong ground shaking in the 1855 Wairarapa Earthquake, *in* Proceedings The 1855 Wairarapa Earthquake symposium, Wellington, 2005.

Fine, I. V., Rabinovich, A. B., Bornhold, B. D., Thomson, R. E., and Kulikov, E. A., 2005, The Grand Banks landslide-generated tsunami of November 18, 1929: preliminary analysis and numerical modeling: Marine Geology, v. 215, no. 1-2, p. 45-57.

Greene, H. G., Maher, N. M., and Paull, C. K., 2002, Physiography of the Monterey Bay National Marine Sanctuary and implications about continental margin development: Marine Geology, v. 181, no. 1-3, p. 55-82.

Grilli, S. T., Taylor, O. D. S., Baxter, C. D. P., and Maretzki, S., 2009, A probabilistic approach for determining submarine landslide tsunami hazard along the upper east coast of the United States: Marine Geology, v. 264, no. 1-2, p. 74-97.

Hampton, M. A., Lee, H. J., and Locat, J., 1996, Submarine Landslides: Reviews of Geophysics, v. 34, p. 33 - 59.

Iglesias, O., Lastras, G., Canals, M., Olabarrieta, M., Gonzalez, M., Aniel-Quiroga, I., Otero, L., Duran, R., Amblas, D., Casamor, J. L., Tahchi, E., Tinti, S., and De Mol, B., 2012, The BIG'95 Submarine Landslide-Generated Tsunami: A Numerical Simulation: Journal of Geology, v. 120, no. 1, p. 31-48.

Labbe, M., Donnadieu, C., Daubord, C., and Hebert, H., 2012, Refined numerical modeling of the 1979 tsunami in Nice (French Riviera): Comparison with coastal data: Journal of Geophysical Research-Earth Surface, v. 117.

Lastras, G., Canals, M., Urgeles, R., Amblas, D., Ivanov, M., Droz, L., Dennielou, B., Fabrés, J., Schoolmeester, T., Akhmetzhanov, A., Orange, D., and García-García, A., 2007, A walk down the Cap de Creus canyon, Northwestern Mediterranean Sea: Recent processes inferred from morphology and sediment bedforms: Marine Geology, v. 246, no. 2-4, p. 176-192.

Micallef, A., Mountjoy, J. J., Canals, M., and Lastras, G., 2012, Deep-Seated Bedrock Landslides and Submarine Canyon Evolution in an Active Tectonic Margin: Cook Strait, New Zealand, *in* Yamada, Y., Kawamura, K., Ikehara, K., Ogawa, Y., Urgeles, R., Mosher, D., Chaytor, J., and Strasser, M., eds., Submarine Mass Movements and Their Consequences, Volume 31, Springer Netherlands, p. 201-212.

Mountjoy, J. J., Barnes, P. M., and Pettinga, J. R., 2009, Morphostructure and evolution of submarine canyons across an active margin: Cook Strait sector of the Hikurangi Margin, New Zealand: Marine Geology, v. 260, no. 1-4, p. 45-68.

Mountjoy, J. J., Micallef, A., Stevens, C. L., and Stirling, M. W., 2013, Holocene sedimentary activity in a non-terrestrially coupled submarine canyon: Cook Strait Canyon system, New Zealand: Deep Sea Research Part II: Topical Studies in Oceanography, no. 0.

Pondard, N., and Barnes, P. M., 2010, Structure and paleoearthquake records of active submarine faults, Cook Strait, New Zealand: Implications for fault interactions, stress loading, and seismic hazard: Journal of Geophysical Research-Solid Earth, v. 115, p. B12320.

Popinet, S., 2003, Gerris: a tree-based adaptive solver for the incompressible Euler equations in complex geometries, J. Comput. Phys., 190, 572–600.

Power, W. L. (compiler), 2013, Review of Tsunami Hazard in New Zealand (2013 Update), GNS Science Consultancy Report 2013/131/ 222 p.

Rahiman, T. I. H., Pettinga, J. R., and Watts, P., 2007, The source mechanism and numerical modelling of the 1953 Suva tsunami, Fiji: Marine Geology, v. 237, no. 1-2, p. 55-70.

Stirling, M. W., McVerry, G., Gersenberger, M., Litchfield, N., Van Dissen, R., Berryman, K., Barnes, P. M., Wallace, L., Villamor, P., Langridge, R., Lamarche, G., Nodder, S., Reyners, M., Bradley, B., Rhoades, D., Smith, W., Nicol, A., Pettinga, J. R., Clark, K., and Jacobs, K., 2012, National seismic hazard model for New Zealand: 2010 update: Bulletin of the Seismological Society of America, v. 102, no. 4, p. 1514-1542.

Strasser, M., Stegmann, S., Bussmann, F., Anselmetti, F. S., Rick, B., and Kopf, A., 2007, Quantifying subaqueous slope stability during seismic shaking: Lake Lucerne as model for ocean margins: Marine Geology, v. 240, no. 1-4, p. 77-97.

Sue, L. P., Nokes, R. I., and Davidson, M. J., 2011, Tsunami generation by submarine landslides: comparison of physical and numerical models. Environmental fluid mechanics, 11(2), 133-165.

Tappin, D. R., Watts, P., and Grilli, S. T., 2008, The Papua New Guinea tsunami of 17 July 1998: anatomy of a catastrophic event: Natural Hazards and Earth System Sciences, v. 8, no. 2, p. 243-266.

Walters, R., Barnes, P., Lewis, K., and Goff, J. R., 2006, Locally generated tsunami along the Kaikoura coastal margin: Part 2. Submarine landslides: New Zealand journal of marine and freshwater research, v. 40, no. 1, p. 17-28.

Ward, S. N., 2001, Landslide tsunami: Journal of Geophysical Research-Solid Earth, v. 106, no. B6, p. 11201-11215.

Watts, P., Grilli, S. T., Kirby, J. T., Fryer, G. J., and Tappin, D. R., 1999, Landslide tsunami case studies using a Boussinesq model and a fully nonlinear tsunami generation model: Nat. Hazards Earth Syst. Sci., v. 3, no. 5, p. 391-402.

Watts, P., Grilli, S. T., Tappin, D. R. & Fryer, G. J., 2005, Tsunami generation by submarine mass failure. II: Predictive equations and case studies: Journal of Waterway, Port, Coastal and Ocean Engineering, v. 131, no. 6**,** p. 298-310.